IFN-Induced Transmembrane Protein 1 Promotes Invasion at Early Stage of Head and Neck Cancer Progression

Hiroko Hatano,[1] Yasusei Kudo,[1] Ikuko Ogawa,[3] Takaaki Tsunematsu,[1] Akira Kikuchi,[2] Yoshimitsu Abiko,[4] and Takashi Takata[1]

Abstract

Purpose: Head and neck squamous cell carcinoma (HNSCC) shows persistent invasion that frequently leads to local recurrence and distant lymphatic metastasis. However, molecular mechanisms associated with invasion of HNSCC remain poorly understood. We identified IFN-induced transmembrane protein 1 (IFITM1) as a candidate gene for promoting the invasion of HNSCC by comparing the gene expression profiles between parent and a highly invasive clone. Therefore, we examined the role of IFITM1 in the invasion of HNSCC.

Experimental Design: IFITM1 expression was examined in HNSCC cell lines and cases by reverse transcription – PCR and immunohistochemistry. IFITM1 overexpressing and knockdown cells were generated, and the invasiveness of these cells was examined by *in vitro* invasion assay. Gene expression profiling of HNSCC cells overexpressing IFITM1 versus control cells was examined by microarray.

Results: HNSCC cells expressed IFITM1 mRNA at higher levels, whereas normal cells did not. By immunohistochemistry, IFITM1 expression was observed in early invasive HNSCC and invasive HNSCC. Interestingly, IFITM1 was expressed at the invasive front of early invasive HNSCC, and higher expression of IFITM1 was found in invasive HNSCC. In fact, IFITM1 overexpression promoted and IFITM1 knockdown suppressed the invasion of HNSCC cells *in vitro*. Gene expression profiling of HNSCC cells overexpressing IFITM1 versus control cells revealed that several genes, including matrix metalloproteinase, were up-regulated in IFITM1 overexpressing cells.

Conclusion: Our findings suggest that IFITM1 plays an important role for the invasion at the early stage of HNSCC progression and that IFITM1 can be a therapeutic target for HNSCC.

Head and neck squamous cell carcinoma (HNSCC) is one of the most common types of human cancer, with an annual incidence of >500,000 cases worldwide (1). The extent of lymph node metastasis is a major determinant in the prognosis of HNSCC. Like most epithelial cancers, HNSCC develops through the accumulation of multiple genetic and epigenetic alterations in a multistep process (2). Recent molecular studies have advanced our understanding of the disease and provided a rationale to develop novel strategies for early detection, classification, prevention, and treatment. Attempts to identify the genes involved in the metastasis are pivotal for the early prediction of HNSCC behavior. The process of metastasis consists of sequential and selective steps, including proliferation, induction of angiogenesis, detachment, motility, invasion into circulation, aggregation and survival in the circulation, cell arrest in distant capillary beds, and extravasation into organ parenchyma (2). We previously established an HNSCC cell line, MSCC-1, from lymph node metastasis (3). Moreover, we isolated a highly invasive clone MSCC-Inv1 from MSCC-1 cells by using an *in vitro* invasion assay device (4). Then, we compared the transcriptional profile of parent cells (MSCC-1) and a highly invasive clone (MSCC-Inv1) by microarray analysis to identify genes that differ in their expression (5). Several genes were selectively overexpressed in the highly invasive clone. Among these genes, the most highly expressed gene was Periostin, and the second was IFN-induced transmembrane protein 1 (IFITM1). In fact, we showed that Periostin promoted invasion both *in vitro* and *in vivo* (5).

IFITM1, also known as 9-27 or Leu13, is a member of the IFN-inducible transmembrane protein family. *IFITM1* gene product was initially identified as Leu13, a leukocyte antigen that is part of a membrane complex involved in the transduction of antiproliferative and homotypic adhesion signals in lymphocytes (6–9). Moreover, IFITM1 is a 17-kDa membrane protein that was inducible on tumor cell lines by IFN-α and usually to a lesser extent by IFN (10). However, there have been a few papers of IFITM1 in cancer, and the role of IFITM1 in cancer is poorly understood. In the present study, therefore, we examined the roles of IFITM1 for HNSCC invasion.

Authors' Affiliations: [1]Department of Oral and Maxillofacial Pathobiology, Division of Frontier Medical Science and [2]Department of Biochemistry, Graduate School of Biomedical Sciences and [3]Center of Oral Clinical Examination, Hiroshima University Hospital, Hiroshima University, Hiroshima, Japan and [4]Department of Biochemistry, School of Dentistry at Matsudo, Nihon University, Tokyo, Japan

Received 10/29/07; revised 1/26/08; accepted 1/29/08.

Grant support: Ministry of Education, Science and Culture of Japan grants-in-aid (Y. Kudo and T. Takata) and Haraguchi Cancer Memorial Foundation grant (Y. Kudo). The costs of publication of this article were defrayed in part by the payment of page charges. This article must therefore be hereby marked *advertisement* in accordance with 18 U.S.C. Section 1734 solely to indicate this fact.

Requests for reprints: Yasusei Kudo or Takashi Takata, Department of Oral and Maxillofacial Pathobiology, Division of Frontier Medical Science, Graduate School of Biomedical Sciences, Hiroshima University, 1-2-3 Kasumi, Minami-ku, Hiroshima 734-8553, Japan. Phone: 81-82-257-5634; Fax: 81-82-257-5619; E-mail: ykudo@hiroshima-u.ac.jp or ttakata@hiroshima-u.ac.jp.

doi:10.1158/1078-0432.CCR-07-4761

Materials and Methods

Cell culture. MSCC-1 and MSCC-Inv1 cells were previously established in our laboratory (3, 4). These cells were maintained in Keratinocyte-SFM (Invitrogen) under a condition of 5% CO_2 in air at 37°C. HNSCC cell lines (HSC2, HSC3, HSC4, Ca9-22, Ho-1-N-1, and Ho-1-U-1) were provided by Japanese Collection of Research Bioresources Cell Bank. They were maintained in RPMI 1640 (Nissui Pharmaceutical Co.) supplemented with 10% heat-inactivated fetal bovine serum (Invitrogen) and 100 units/mL penicillin-streptomycin (Life Technologies) under conditions of 5% CO_2 in air at 37°C. Normal oral epithelial cells and gingival fibroblasts were obtained from oral mucosa or gingival tissues using standard explant techniques (11). These tissues were obtained from routine dental surgery in the Department of Oral Surgery, Hiroshima University Hospital. Normal oral epithelial cells were routinely maintained in Keratinocyte-SFM (Life Technologies-Bethesda Research Laboratories), and gingival fibroblasts were maintained in DMEM supplement with 10% fetal bovine serum. For growth assay, 5000 cells were plated on 24-well plates (Falcon), and trypsinized cells were counted by Cell Counter (Coulter Z1) at 4 d.

Reverse transcription–PCR. Total RNA was isolated from cultures of confluent cells using the RNeasy mini kit (Qiagen). Preparations were quantified, and their purity was determined by standard spectrophotometric methods. cDNA was synthesized from 1 μg total RNA according to the ReverTra Dash (Toyobo Biochemicals). Primer sequences were listed in Table 1A. Aliquots of total cDNA were amplified with Go Taq Green Master Mix (Promega), and amplifications were done in a PC701 thermal cycler (Astec) for 25 (IFITM1 and CD81) or 30 [glyceraldehyde-3-phosphate dehydrogenase (GAPDH), βTrcp-1, βTrcp2, ZNF236, matrix metalloproteinase 13 (MMP13), and MMP12] cycles after an initial 30-s denaturation at 94°C, annealed for 30 s at 60°C, and extended for 1 min at 72°C in all primers. The amplification reaction products were resolved on 1.5% agarose/TAE gels (Nacalai Tesque, Inc.), electrophoresed at 100 mV, and visualized by ethidium-bromide staining.

Western blot analysis. Western blotting was carried out as we described previously (5). An anti-IFITM1 polyclonal antibody (Boster Biological Technology Ltd.), anti-CD81 monoclonal antibody (BD Biosciences), anti-FLAG monoclonal antibody (Sigma), and anti-Cul1 polyclonal antibody (Zymed) were used. Thirty micrograms of protein were subjected to 10% PAGE followed by electroblotting onto a nitrocellulose filter. For detection of the immunocomplex, the enhanced chemiluminescence Western blotting detection system (Amersham) was used. We used Cul1 expression as a loading control. Cul1 is one of the components of SCF ubiquitin ligase complex and is expressed at a relatively constant rate and expression level does not change after drug treatment. For detecting CD81, we performed immunoprecipitation with anti-CD81 antibody followed by immunoblotting analysis with a same antibody.

Tissue samples. Tissue samples of HNSCC were retrieved from the Surgical Pathology Registry of Hiroshima University Hospital after approval by the Ethical Committee of our institutions. Twenty cases of frankly invasive HNSCC, 11 early invasive HNSCC, and 10 normal oral mucosal tissues were used in this study. 10% buffered, formalin-fixed, and paraffin-embedded tissues were used for immunohistochemical examination. The histologic grade and stage of tumor were classified according to the criteria of the Japan Society for Head and Neck Cancer.

Immunohistochemical staining. Immunohistochemical detection of IFITM1 in HNSCC cases was done on 4.5-μm sections mounted on

Table 1.

A. Oligonucleotide primer sequences used in the RT-PCR

RT-PCR primer set	Sequence	Product length (bp)
IFITM1	F 5′-atgtcgtctggtccctgttc-3′ R 5′-gtcatgaggatgcccagaat-3′	300
CD81	F 5′-agatcgccaaggatgtgaag-3′ R 5′-cctccttgaagaggttgctg-3′	213
GAPDH	F 5′-tccaccaccctgttgctgta-3′ R 5′-accacagtccatgccatcac-3′	450
βTrcp-1	F 5′-aacggaaactctcagcaagc-3′ R 5′-tggcatccaggtatgacaga-3′	240
βTrcp-2	F 5′-aaaccagcctggaatgtttg-3′ R 5′-cagtccattgctgaagcgta-3′	197
ZNF236	F 5′-agctcactcaaaggcggtaa-3′ R 5′-tatagtcctgtcggggttcg-3′	201
MMP13	F 5′-ttgagctggactcattgtcg-3′ R 5′-ggagcctctcagtcatggag-3′	171
MMP12	F 5′-acacatttcgcctctctgct-3′ R 5′-ccttcagccagaagaacctg-3′	192

B. Oligonucleotide sequences used for siRNA

shIFITM1	
1	F 5′-TGCTGTTCAGTTTCTCAGAAGTGTGTGTTTTGGCCACTGACTGACACACACTTGAGAAACTGAA-3′
	R 5′-CCTGTTCAGTTTCTCAAGTGTGTGTCAGTCAGTGGCCAAAACACACACTTCTGAGAAACTGAAC-3′
2	F 5′-TGCTGACCAGTGACAGGATGAATCCAGTTTTGGCCACTGACTGACTGGATTCACTGTCACTGGT-3′
	R 5′-CCTGACCAGTGACAGTGAATCCAGTCAGTCAGTGGCCAAAACTGGATTCATCCTGTCACTGGTC-3′
3	F 5′-TGCTGTAATATGGTAGACTGTCACAGGTTTTGGCCACTGACTGACCTGTGACACTACCATATTA-3′
	R 5′-CCTGTAATATGGTAGTGTCACAGGTCAGTCAGTGGCCAAAACCTGTGACAGTCTACCATATTAC-3′
shCD81	
1	F 5′-TGCTGAGATACAGGAGGTTGGTGGTCGTTTTGGCCACTGACTGACGACCACCACTCCTGTATCT-3′
	R 5′-CCTGAGATACAGGAGTGGTGGTCGTCAGTCAGTGGCCAAAACGACCACCAACCTCCTGTATCTC-3′
2	F 5′-TGCTGCATACACGCCACCTACATGTGGTTTTGGCCACTGACTGACCACATGTATGGCGTGTATG-3′
	R 5′-CCTGCATACACGCCATACATGTGGTCAGTCAGTGGCCAAAACCACATGTAGGTGGCGTGTATGC-3′
3	F 5′-TGCTGTTGTGATTACAGTTGAAGGCGGTTTTGGCCACTGACTGACCGCCTTCATGTAATCACAA-3′
	R 5′-CCTGTTGTGATTACATGAAGGCGGTCAGTCAGTGGCCAAAACCGCCTTCAACTGTAATCACAAC-3′

silicon-coated glass slides, using a streptavidin–biotin peroxidase technique, as described previously (12).

Generation of IFITM1-overexpressing HNSCC cells. Human *IFITM1* cDNA was isolated from the cDNA by reverse transcription–PCR (RT-PCR) using sense and antisense primers. Human *IFITM1* cDNA was then subcloned by insertion into the *Eco*RI/*Bam*HI restriction site of pBICEP-CMV-2 (Sigma). The IFITM1–pBICEP–CMV-2 plasmid or the vector alone was introduced into Ca9-22 cells, and the stable

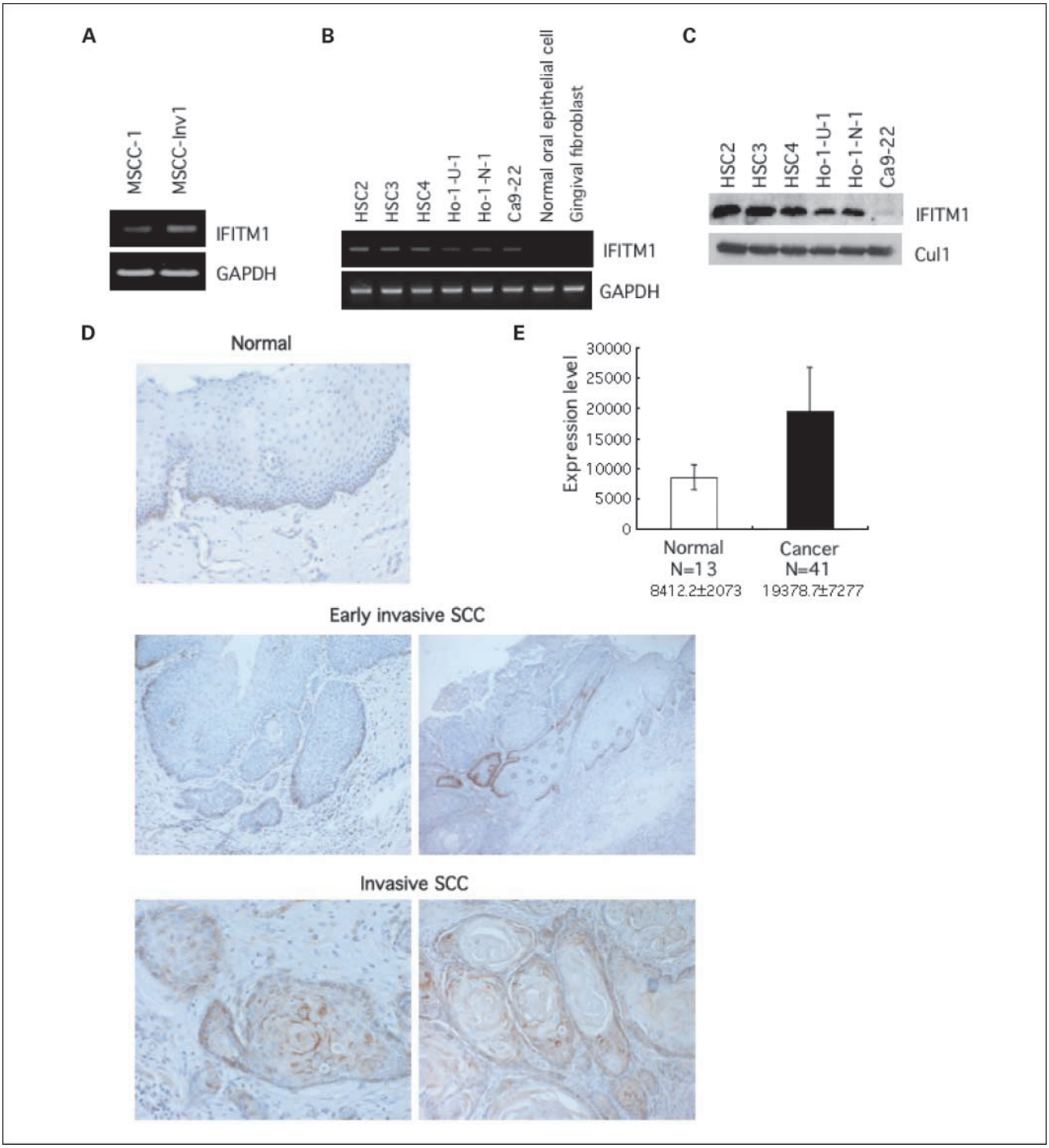

Fig. 1. Overexpression of IFITM1 in HNSCC. *A,* confirmation of higher expression of IFITM1 mRNA in the highly invasive clone by RT-PCR. *B,* expression of IFITM1 mRNA in six HNSCC cell lines, normal oral epithelial cells, and gingival fibroblasts. Expression of IFITM1 mRNA was done by RT-PCR. *C,* expression of IFITM1 protein in six HNSCC cell lines by Western blot analysis. Cul1 expression was used as a loading control. *D,* expression of IFITM1 was examined by immunohistochemistry in normal oral mucosae (Normal, 40×), early invasive HNSCC (early invasive SCC, 40×), and invasive HNSCC (SCC, 40×). Representative cases of IFITM1 expression. Scale bar; 100 μm. *E,* total RNA from 41 primary HNSCC and 13 normal tissues was labeled and hybridized to Affymetrix U133A Gene Chips, as previously reported (17). Graph shows the signal intensity of IFITM1 in 41 HNSCC and 13 normal tissues in microarray analysis in normal and HNSCC tissues. The average of signal intensity of IFITM1 is shown at the bottom of the graph. $P < 0.05$ when compared with normal tissues.

clones were obtained by G418 selection (500 μg/mL, Life Technologies) in the culture medium. We obtained pool and four stable clones. Cell transfection was done using FuGENE 6 HD (Roche) according to the manufacture's instruction.

In vitro *invasion assay.* *In vitro* invasion assay was done as described previously (4, 13). Briefly, invasion was measured by use of a 24-well cell culture insert with 8-μm pores (3097, Falcon, Becton Dickinson). The filter was coated with 50 μl of Matrigel (Becton Dickinson), which was reconstituted basement membrane substance. The lower compartment contained 0.5 mL of serum-free medium. After trypsinization, 1.5×10^5 cells were resuspended in 100 μL of serum-free medium and placed in the upper compartment of the cell culture insert for 24 h. To examine the invasiveness, penetrated cells onto the lower side of the filter were fixed with formalin and stained with hematoxylin. We assayed thrice.

Wound healing assay. For the wounding healing experiment, cells were seeded on six-well plates and cells were allowed to grow to complete confluence. Subsequently, a plastic pipette tip was used to scratch the cell monolayer to create a cleared area, and the wounded cell layer was washed with fresh medium to remove loose cells. Immediately after scratch wounding (0 h) and after incubation of cells at 37°C for 24 h, phase-contrast images (10× field) of the wound healing process were photographed digitally with an inverted microscope. The distance of the wound areas (cell-free area) were measured on the images, set at 100% for 0 h, and the mean percentage of cell-free area was calculated.

RNA interference experiments. Short hairpin RNAs (shRNA) were designed based on the prediction of publicly available prediction programs (14), which are summarized in Table 1B. shRNAs were cloned into the transient microRNA expression vector pcDNA6.2-GW/emGFP/miR (Invitrogen), which coexpresses the shRNA surrounded by miR-155–flanking sequences together with emGFP. Logarithmically growing Ca9-22 and HSC2 cells were seeded at a density of 10^5 cells per 6-cm dish and were transfected. After 48 h of transfection, we treated blasticidin for 10 d. After selection, we obtained the stably shRNA-expressing cells. si-miR-neg, provided by Invitrogen, has an insert that can form a hairpin structure that is processed into mature microRNA, but it is predicted not to target any known vertebrate gene (according to Invitrogen). Transfection efficiency was checked by GFP expression under UV microscopy and by RT-PCR.

For knockdown of β-Trcp, we used the small interfering RNA (siRNA) oligos. The siRNA oligos used for both β-Trcp1 and β-Trcp2 silencing were 21-bp synthetic molecules (Dharmacon Research) corresponding to nt 407-427 of human β-Trcp1 and 161-181 of human β-Trcp2 (AB033279; ref. 15). A 21-nt siRNA duplex corresponding to a nonrelevant F-box protein gene was used as a control. Logarithmically growing Ca9-22 cells were seeded at a density of 10^5cells per 6-cm dish

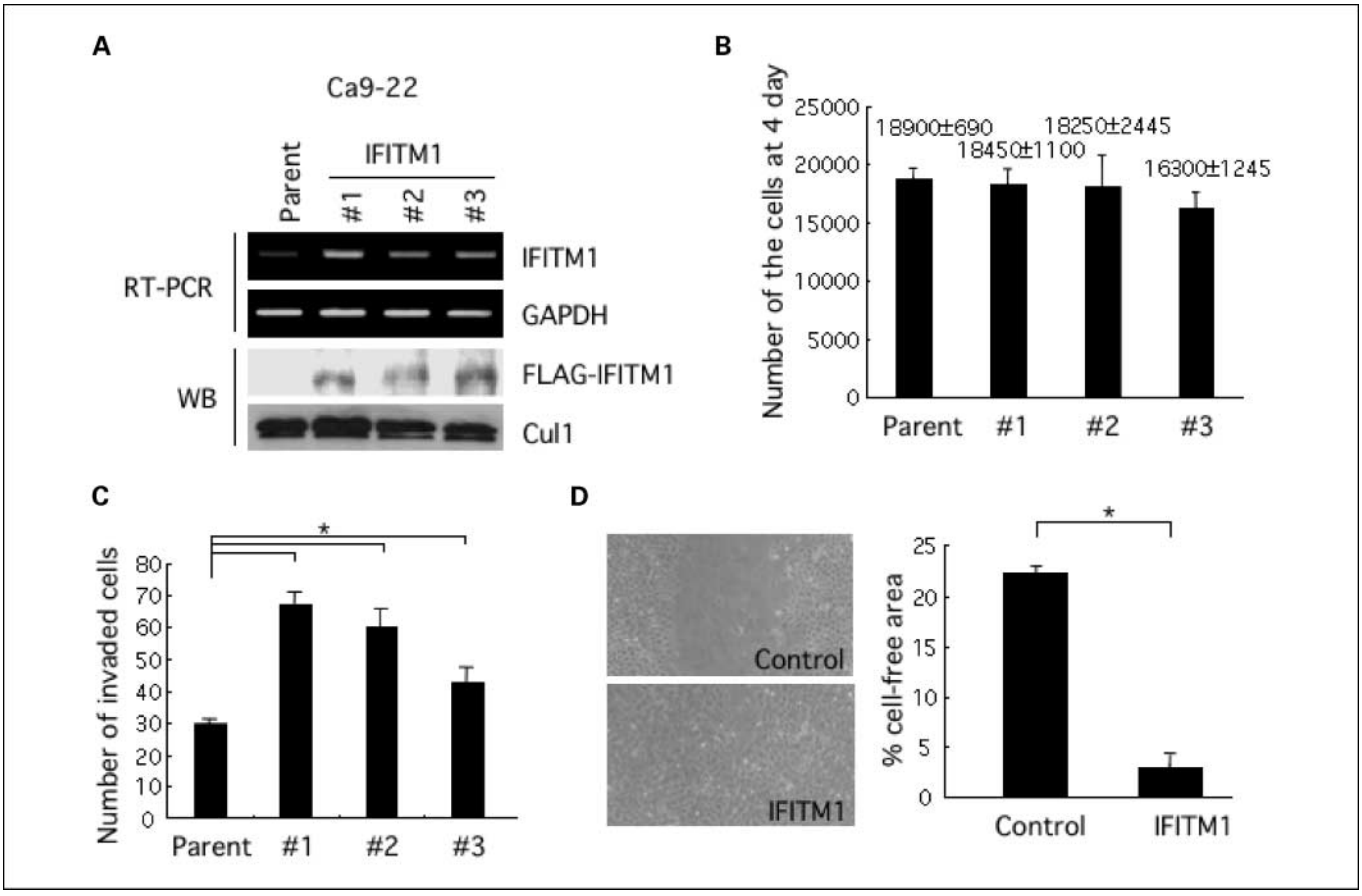

Fig. 2. IFITM1 promotes the invasion of HNSCC cells. *A,* generation of IFITM1-overexpressing cells. Ca9-22 cells were engineered to overexpressing IFITM1 by transfection with pBICEP – CMV-2 – IFITM1. We obtained three stable clones of IFITM1-overexpressing cells. Ectopic expression of IFITM1 was examined by immunoblotting with anti-FLAG antibody. The whole lysates from all samples were blotted with Cul1 for a loading control. *B,* cell proliferation of IFITM1-overexpressing HNSCC cells. Cells were plated on 24-well plates, and trypsinized cells were counted by Cell Counter at 4 d. *C,* invasion of IFITM1-overexpressing HNSCC cells. The invasiveness of the cells was determined by *in vitro* invasion assay. 1.5×10^5 cells were placed in the upper compartment of the cell culture insert for 24 h. To examine the invasiveness, penetrated cells onto the lower side of the filter were fixed with formalin and stained with hematoxylin. We assayed thrice. *, $P < 0.05$ when compared with parent cells. *D,* migration of IFITM1-overexpressing HNSCC cells. We used one of stable clones for wound healing assay. Migration of the cells was determined by wound healing assay. At 24 h after scratching the cells, phase-contrast images (10× field) of the wound healing process were photographed digitally with an inverted microscope. The distance of the wound areas was measured on the images, set at 100% for 0 h, and the mean percentage of the total distances of the wound areas was calculated. *, $P < 0.05$ when compared with control cells.

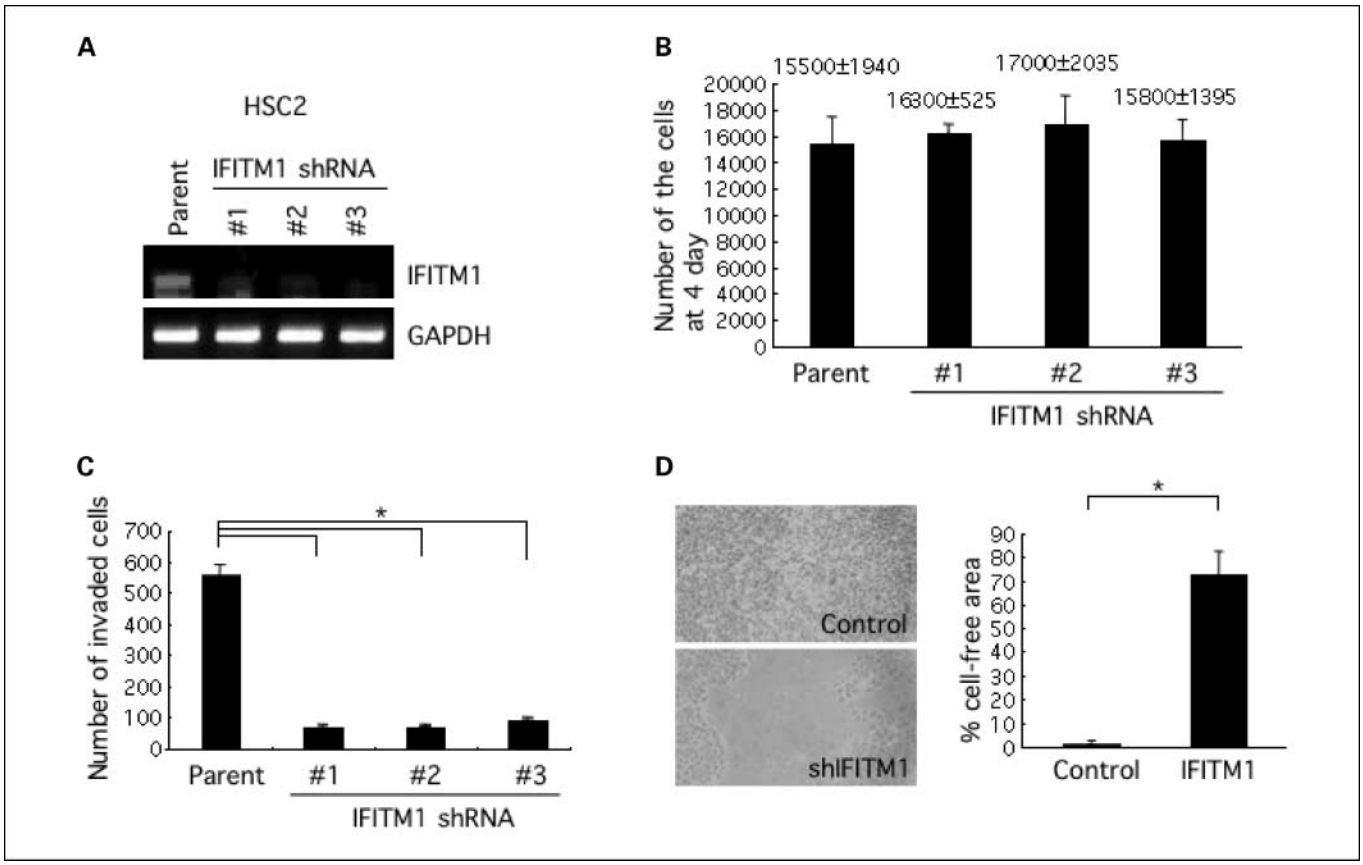

Fig. 3. IFITM1 shRNA inhibited the invasion of HNSCC cells. *A,* three different IFITM1 shRNAs were stably transfected in HSC2 cells. After transfection, we treated blastidin for selection. IFITM1 mRNA expression is examined by RT-PCR. GAPDH expression was used as a loading control. *B,* cell proliferation of IFITM1 shRNA transfected cells. Cells were plated on 24-well plates and trypsinized cells were counted by Cell Counter at 4 d. *C,* invasion of IFITM1 shRNA transfected cells. The invasiveness of the cells was determined by *in vitro* invasion assay. 1.5×10^5 cells were placed in the upper compartment of the cell culture insert for 24 h. To examine the invasiveness, penetrated cells onto the lower side of the filter were fixed with formalin and stained with hematoxylin. We assayed thrice. $^*P < 0.05$ when compared with parent cells. *D,* Migration of IFITM1 shRNA transfectd HNSCC cells. We used one of stable clones for wound healing assay. Migration of the cells was determined by wound healing assay. At 18 h after scratching the cells, phase-contrast images (10× field) of the wound healing process were photographed digitally with an inverted microscope. The distance of the wound areas were measured on the images, set at 100% for 0 h, and the mean percentage of the total distances of the wound areas were calculated. $^*P < 0.05$ when compared with control cells.

and transfected with oligos twice (at 24 and 48 h after replating) using Oligofectamine (Invitrogen) as described (16). Forty-eight hours after the last transfection, lysates were prepared and analyzed by SDS-PAGE and immunobloting.

Gene array analysis. The human focus array using the system containing 50,000 gene probes was used for comparing the transcriptional profiles between IFITM1 overexpressing Ca9-22 cells and control Ca9-22 cells. This array contains a broad range of genes derived from publicly available, well-annotated mRNA sequences. Total RNA was isolated from cultures of confluent cells using the RNeasy Mini kit (Qiagen) according to the manufacturer's instructions. Preparations were quantified, and their purity was determined by standard spectrophotometric methods. Data were expressed as the average differences between the perfect match and mismatch probes for the IFITM1 gene.

Statistical analysis. Student's *t* test was used to analyze the difference between two groups. A P value < 0.05 was required for significance.

Results

IFITM1 overexpression is frequently found in HNSCC. We previously identified IFITM1 as an invasion-promoting factor of HNSCC by comparing the transcriptional profile of parent HNSCC cells (MSCC-1) and a highly invasive clone (MSCC-Inv1; ref. 5). The finding of higher expression of IFITM1 in the highly invasive clone than the parent cells was confirmed by RT-PCR (Fig. 1A). Next, we examined the IFITM1 mRNA in six HNSCC cell lines, normal oral epithelial cells, and normal gingival fibroblasts. IFITM1 mRNA expression was observed in all HNSCC cell lines, but not in normal epithelial cells and fibroblasts (Fig. 1B). IFITM1 protein expression was examined by Western blot analysis in HNSCC cells, and anti-IFITM1 antibody recognized IFITM1 protein (Fig. 1C). IFITM1 protein expression was well conceited with mRNA expression level in most cell lines. However, IFITM1 protein expression is low in Ca9-22 cells with significant amount of IFITM1 mRNA. This discrepancy may be accounted for by two possibilities; (a) mRNA expression level was examined by RT-PCR not by quantitative method and (b) protein level was decreased by translational modification. By using this antibody, we examined the expression of IFITM1 by immunohistochemistry to know the localization of IFITM1 in HNSCC. Twenty cases of frankly invasive HNSCC, 11 early invasive HNSCC, and 10 normal oral mucosal tissues were used in this study. Early invasive cancer shows earliest moment of invasion (limited to the mucosal or submucosal area without invading the underlying muscle or bone tissues) and is also known as "superficially invasive" or "microinvasive." In normal oral epithelium, only basal cells slightly expressed IFITM1 in their cytoplasm and membrane

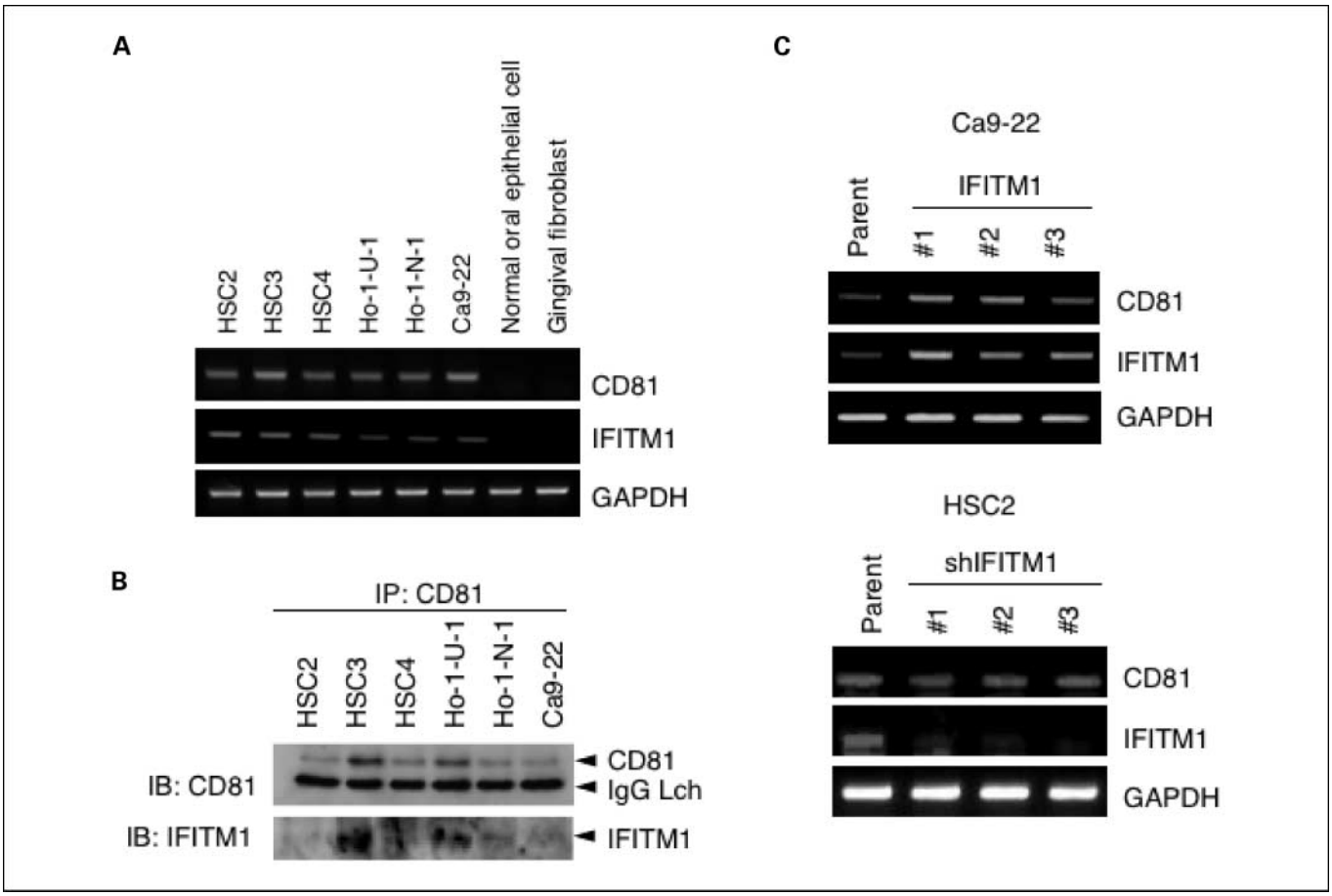

Fig. 4. Correlation between IFITM1 and CD81 in HNSCC cells. *A,* expression of CD81 mRNA in six HNSCC cell lines, normal oral epithelial cells, and gingival fibroblasts. Expression of CD81 mRNA was done by RT-PCR. The picture of IFITM1 and GAPDH mRNA expression is same as Fig. 1B. *B,* Expression of CD81 protein in 6 HNSCC cell lines by immunoprecipitation and immunoblotting of CD81. CD81 was precipitated from lysates with the use of monoclonal antibodies specific CD81 and immunoblots was probed with CD81 and IFITM1 antibodies. IgG Lch, IgG light chain; IP, immunoprecipitation; and IB, immunoblotting. *C,* CD81 expression was examined in IFITM1-overexpressing and IFITM1 knockdown cells by RT-PCR. The picture of IFITM1 and GAPDH expression in IFITM1-overexpressing and IFITM1 knockdown cells is same as Figs. 2A and 3A, respectively. Top, CD81 expression in stable clones of IFITM1-overexpressing cells; bottom, CD81 expression in IFITM1 shRNA-treated cells.

(Fig. 1D). In early invasive HNSCC, surrounding cells in cancer nests of invasive front expressed IFITM1 at higher levels in comparison with basal cells in normal epithelium (Fig. 1D). In frankly invasive HNSCC, cancer cells expressed IFITM1 at higher levels in their cytoplasm and membrane (Fig. 1D). As all cancer cases expressed IFITM1 at higher levels, we could not compare with clinicopathologic findings, including histologic differentiation and metastasis. Thus, high expression of IFITM1 was focally observed in invasive front of early invasive HNSCC and diffusely observed in invasive HNSCC. As early invasive HNSCC is considered as a tumor at the early stage of cancer progression, this finding suggests that IFITM1 may be involved in the invasion at the early stage of HNSCC progression. For further evaluation of IFITM1 expression in patients with HNSCC, we compared the expression in a previously published microarray dataset of 41 HNSCC patients and 13 normal controls (17). Similar to our data, IFITM1 was expressed at higher levels in HNSCC tissues, in comparison with normal oral mucosal tissues (Fig. 1E).

IFITM1 is involved in the invasion of HNSCC cells. To show the involvement of IFITM1 in the invasion of HNSCC, we generated the IFITM1-overexpressing cells. We transfected IFITM1 into Ca9-22 cells that showed low expression of IFITM1. Then, we obtained three stable clones of IFITM1-overexpressing cells (Fig. 2A). IFITM1 overexpression did not change the cell proliferation (Fig. 2B). We compared the invasiveness between control and IFITM1-overexpressing HNSCC cells. By *in vitro* invasion assay, IFITM1 overexpression enhanced the invasion (Fig. 2C). Moreover, IFITM1 overexpression enhanced the migration by wound healing assay (Fig. 2D). To confirm the IFITM1-mediated invasion and migration of HNSCC cells, we examined the knockdown of IFITM1 by using shRNAs in HSC2 cells with high expression of IFITM1. We designed three different shRNAs (1, 2, and 3) and transfected them into HSC2 cells. All shRNAs reduced the IFITM1 expression (Fig. 3A). IFITM1 shRNAs did not influence cell proliferation (Fig. 3B), but IFITM1 shRNAs remarkably inhibited invasion and migration of HNSCC cells (Fig. 3C and D).

CD81 is involved in the invasion of HNSCC cells. CD81 is a widely expressed cell-surface protein involved in an astonishing variety of biological responses (18). CD81 associates on the surface of B cells in a molecular complex that includes the B-cell–specific molecules CD19 and CD21 and Leu-13/IFITM1 (18). As we thought that CD81 may be involved in IFITM1-mediated invasion of HNSCC cells, we examined the correlation between CD81 and IFITM1 expression in HNSCC cells. First, we examined the expression of CD81 mRNA in HNSCC cell

lines and normal cells. In similar to IFITM1 expression, CD81 expression was observed only in HNSCC cells, but not in normal oral epithelial cells and gingival fibroblasts (Fig. 4A). Expression of CD81 protein was observed in all HNSCC cells, and CD81 expression was not correlated with IFITM1 expression (Fig. 4B). However, the interaction between CD81 and IFITM1 was detected in all HNSCC cells (Fig. 4B). To check the correlation between IFITM1 and CD81, we examined the CD81 expression in IFITM1 overexpressing and IFITM1 knockdown cells. Although IFITM1 overexpression enhanced CD81 expression, IFITM1 knockdown did not affect CD81 expression (Fig. 4C). To know the role of CD81 for the invasion of HNSCC cells, we examined the knockdown of CD81 in HSC2 cells by using shRNA. We designed three different shRNAs (1, 2, and 3) and transfected them into HSC2 cells. All shRNAs reduced CD81 expression, and reduced expression of IFITM1 was observed in 2 of 3 clones (#1 and #3; Fig. 5A). In similar to the phenotype of IFITM1 knockdown cells, CD81 knockdown remarkably inhibited the invasion of HNSCC cells (Fig. 5B). Moreover, we transfected three different CD81 shRNA into the IFITM1 overexpressing HNSCC cells (Fig. 5C). CD81 knockdown inhibited the IFITM1 enhanced invasion of HNSCC cells, indicating that CD81 may be involved in the invasion of HNSCC cells (Fig. 5C).

Recent studies have shown that during embryogenesis, BMP4 and Wnt/β-catenin signaling were able to control the

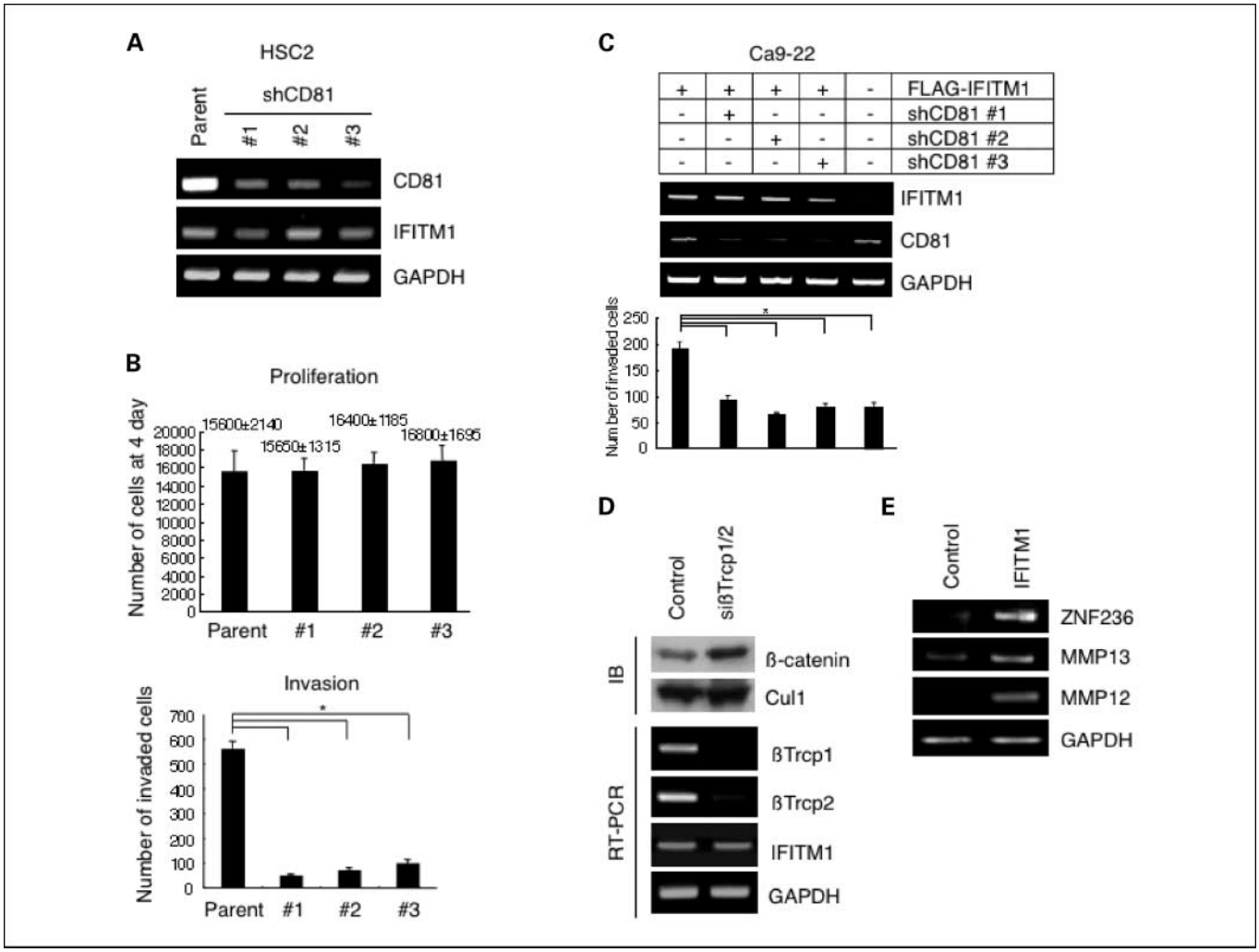

Fig. 5. CD81 is involved in the invasion of HNSCC cells. *A,* three different CD81 shRNAs were stably transfected in HSC2 cells. After transfection, we treated blasticidin for selection. CD81 and IFITM1 mRNA expression is examined by RT-PCR. GAPDH expression was used as a loading control. *B,* cell proliferation of CD81 shRNA-treated cells (top). Cells were plated on 24-well plates, and trypsinized cells were counted by Cell Counter at 0 and 4 d. We defined 1 as a number of cells at 0 d and calculated the fold change of number of cells at 4 d. Invasion of CD81 shRNA-treated cells (bottom). The invasiveness of the cells was determined by *in vitro* invasion assay. 1.5×10^5 cells were placed in the upper compartment of the cell culture insert for 24 h. To examine the invasiveness, penetrated cells onto the lower side of the filter were fixed with formalin and stained with hematoxylin. We assayed thrice. $^*P < 0.05$ when compared with parent cells. *C,* we examined the cotransfection of CD81 shRNA into IFITM1 transfected HNSCC cells. Three different CD81 shRNAs (1, 2, and 3) were transiently transfected into IFITM1-overexpressing Ca9-22 cells. IFITM1 and CD81 expression was examined by RT-PCR (top). GAPDH was used as a control. The invasiveness of the cells was determined by *in vitro* invasion assay (bottom). 1.5×10^5 cells were placed in the upper compartment of the cell culture insert for 36 h. To examine the invasiveness, penetrated cells onto the lower side of the filter were fixed with formalin and stained with hematoxylin. We assayed thrice. $^*P < 0.05$ when compared with IFITM1 overexpressing cells without shCD81 translation. *D,* IFITM1 is not induced by Wnt/β-catenin signaling pathway. We treated β-Trcp1/2 siRNA in HNSCC cells. A 21-nt duplex corresponding to a nonrelevant F-box protein gene was used as a control. β-Trcp1/2 siRNA induced down-regulation of β-Trcp1 and β-Trcp2 mRNA and accumulation of β-catenin protein. In this β-Trcp1/2 siRNA-treated cells, IFITM1 mRNA was examined by RT-PCR. GAPDH was used as a control for RT-PCR. Cul1 was used as a loading control for Western blot analysis. *E,* gene expression profiles of control and IFITM1-overexpressing HNSCC cells. ZNF236, MMP13, and MMP12 were up-regulated in IFITM1-overexpressing cells (Table 1). We confirmed the expression of ZNF236, MMP13, and MMP12 mRNA in IFITM1 HNSCC-overexpressing cells by RT-PCR. GAPDH expression was used as a loading control.

Table 2. List of genes up-regulated by IFITM1 (over 6-fold) in Ca9-22 cells

Ratio (IFITM1/ control)	Control normalized	IFITM1 normalized	Genbank	Common	Description
65.7	0.052373156	3.438695	AK000847	*ZNF236*	Zinc finger protein 236
23.5	0.040916532	0.95997965	AA053711	*EDIL3*	EGF-like repeats and discoidin I-like domains 3
19.1	0.29541734	5.6548567	NM_002427	*MMP13*	Matrix metallopeptidase 13 (collagenase 3)
19.1	0.02700491	0.5164415	AI681013	*PRDM2*	PR domain containing 2, with ZNF domain
12.5	0.039279867	0.490441	NM_024722	*ACBD4*	Acyl-coenzyme A binding domain containing 4
10.1	0.049918167	0.50318635	U50748	*LEPR*	Leptin receptor
9.6	0.06628478	0.6377772	D49958	*GPM6A*	Glycoprotein M6A
8.7	0.06382978	0.556207	AF230398	*TRIM23*	Tripartite motif-containing 23
8.2	0.18903437	1.5421872	NM_002426	*MMP12*	Matrix metallopeptidase 12 (macrophage elastase)
7.5	0.063011445	0.47004843	AK026191	*DDAH2*	Dimethylarginine dimethylaminohydrolase 2
7.3	0.7765958	5.682895	NM_005410	*SEPP1*	Selenoprotein P, plasma, 1
7.0	0.106382966	0.7427989	NM_004585	*RARRES3*	Retinoic acid receptor responder (tazarotene induced) 3
6.9	0.06873976	0.47667605	AF196478	*ANXA10*	Annexin A10
6.8	0.2119476	1.4453225	AF096296	*CCL26*	Chemokine (C-C motif) ligand 26
6.6	0.08428806	0.55365795	AL034410	*PCNAP*	proliferating cell nuclear antigen pseudogene
6.6	0.091653034	0.60056084	BF939489	*GPM6A*	Glycoprotein M6A
6.5	0.117839605	0.7687994	AV747166	*PARP11*	Poly (ADP-ribose) polymerase family, member 11
6.3	0.29214403	1.8307419	AL541302	*SERPINE2*	Serpin peptidase inhibitor, clade E (nexin, plasminogen activator inhibitor type 1), member 2
6.0	0.07774141	0.46902883	AL037998		CDNA FLJ30740 fis, clone FEBRA2000319

level of expression of IFITM1 and that IFITM1 is induced by activation of the Wnt/β-catenin signaling during intestinal tumorigenesis (19, 20). Activation of Wnt signaling pathway leads to inhibition of β-catenin degradation by decreasing the ability of GSK3β to phosphorylate β-catenin, and stabilization of β-catenin enhances the interaction with members of the T-cell factor/lymphoid enhancer factor (Tcf/Lef) family of transcription factors (21). In the absence of a Wnt signal, β-catenin is phosphorylated by a multimolecular complex consisting GSK3, APC and AXIN, and then the phosphorylated β-catenin is recognized and ubiquitinated by E3 ubiquitin ligase complex, $SCF^{\beta\text{-Trcp}}$ (22). Therefore, we examined whether overexpression of IFITM1 in HNSCC cells is induced by activation of the Wnt/β-catenin signaling. β-Trcp siRNA treatment induced β-catenin accumulation, indicating the activation of the Wnt/β-catenin signaling (Fig. 5D). However, IFITM1 was not up-regulated in β-Trcp siRNA-treated HNSCC cells (Fig. 5D).

IFITM1 overexpression induces up-regulation of MMP. To know the mechanism of IFITM1 for the invasion of HNSCC cells, we compared the gene transcriptional profiles of control and IFITM1 overexpressing HNSCC cells. By microarray analysis, several genes were selectively overexpressed in IFITM1 overexpressing HNSCC cells (Table 2). Among these genes, ZNF236 was the most highly expressed gene. ZNF236, a novel Kruppel-like zinc-finger gene, was initially identified by its glucose-regulated expression in human mesangial cells using mRNA differential display (23). In addition, MMP13 and MMP12 were up-regulated in IFITM1 overexpressing HNSCC cells. Certain aspects of MMP involvement in tumor metastasis, such as tumor-induced angiogenesis, tumor invasion, and establishment of metastatic foci at the secondary site, have received extensive attention that resulted in an overwhelming amount of experimental and observational data in favor of critical roles of MMPs in these processes (24). Highly expression of ZNF236, MMP13 and MMP12 in IFITM1 overexpressing HNSCC cells was confirmed by RT-PCR (Fig. 5E).

Discussion

We previously identified several genes, which encode secretary or cell surface proteins implicated in invasion, cell adhesion, angiogenesis and growth factor, as a candidate gene for the invasion of HNSCC by comparing the gene expression profiles between parent HNSCC cells and a highly invasive clone using microarray analysis (5). IFITM1 was the second of overexpressed genes in highly invasive clones, and we considered it as a novel candidate gene for HNSCC invasion. As we expected, IFITM1 overexpression promoted the invasion and migration of HNSCC cells *in vitro* (Fig. 2). These findings are consistent with the recent report that IFITM1 modulates the invasiveness of gastric cancer cells (25). We also found that high expression of IFITM1 was focally observed in invasive front of early invasive HNSCC and diffusely observed in invasive HNSCC by immunohistochemical analysis, suggesting that IFITM1 may be involved in the invasion at the early stage of HNSCC progression. This observation is consistent with recent report that expression of several members of the IFITM family was up-regulated in early and late intestinal neoplasms by using different mouse models of Apc inactivation and human colon tumor samples and that up-regulation of the *IFITM* genes seems to be an early event in β-catenin intestinal tumorigenesis (20). We suggest that IFITM1 may be involved in the initial step of invasion, such as the degradation of the basement membrane and the interstitial extracellular matrix, which results in cellular infiltration into the adjacent tissue. In our microarray analysis, we identified Periostin as the most highly expressed gene in highly invasive clones (5). In fact, we showed that Periostin dramatically enhanced invasion, anchorage-independent growth both *in vitro* and *in vivo*, and that Periostin overexpression was well correlated with poorly differentiation and metastasis in HNSCC cases by immunohistochemistry (5). We suggested that Periostin overexpression might be a late event, such as the aggressive invasion into surrounding tissues, invasion into circulation, and extravasation into organ parenchyma

in HNSCC progression. Overall, IFITM1 and Periostin can be a marker for predicting the invasion of HNSCC at the early and late stage of HNSCC progression, respectively.

To know the mechanism of IFITM1 for invasion of HNSCC cells, we compared the gene expression profiles between control and IFITM1 overexpressing HNSCC cells. IFITM1 overexpression enhanced MMP12 and MMP13 expression in HNSCC cells (Fig. 5E and Table 1), suggesting that IFITM1 enhanced invasion of HNSCC cells through the activation of certain type of MMP. Previous studies showed that IFITM1 associates with CD81 and make a complex with CD19 and CD21 (18). In addition, it has been reported that constitutive up-regulation of CD81 is associated with an increased growth rate and tumor progression in a mouse model of skin tumor (26). Therefore, we asked whether CD81 was involved in the IFITM1-induced invasion of HNSCC cells or not. In similar to IFITM1 expression, CD81 expression was observed in HNSCC cells, but not in normal cells (Fig. 4A). Interestingly, IFITM1 overexpression enhanced CD81 expression (Fig. 4B) and knockdown of CD81 inhibited the invasion of HNSCC cells in similar to IFITM1 knockdown (Fig. 5B). Moreover, CD81 knockdown abolished IFITM1-induced invasion of HNSCC cells (Fig. 5C). Although these findings suggest that CD81 may be involved in the invasion of HNSCC, the association between IFITM1 and CD81 for the invasion of HNSCC cells is still unclear. As CD81 is associated with integrins ($\alpha6\beta1$ and $\alpha3\beta1$) in HeLa cells (27), CD81 induced invasion may be associated with certain types of integrins. It is also known that CD81 is considered a putative receptor for hepatitis C virus (28). Therefore, this finding raises the possibility that unknown ligand may bind to CD81 and may be involved in CD81-induced invasion. To show the detailed molecular mechanisms of IFITM1 and CD81 for cancer invasion, further studies will be required.

In the present study, highly expression of IFITM1 was observed in all HNSCC cancer cell lines and invasive HNSCC cancer cases. Up-regulation of IFITM1 was observed in colon, rectal, stomach, and lung cancers by large-scale analysis of IFITM expression (24). Therefore, up-regulation of IFITM1 may be a common event in the progression of various cancers. Recent studies have shown that, during embryogenesis, BMP4 and Wnt/β-catenin signaling were able to control the level of expression of IFITM1 and that IFITM1 is induced after activation of the Wnt/β-catenin signaling during intestinal tumorigenesis (19, 20). However, IFITM1 was not up-regulated by activation of the Wnt/β-catenin signaling in HNSCC cells (Fig. 5D). To clarify the mechanism of up-regulation of IFITM1 will require further studies. In conclusion, our studies have revealed a critical role of IFITM1 for the invasion at the early stage of HNSCC progression. These findings provide new and important information on the progression of HNSCC and suggest that IFITM1 could be used as a novel molecular target for therapy of HNSCC patients.

Disclosure of Potential Conflicts of Interest

No potential conflicts of interest were disclosed.

Acknowledgments

We thank Dr. P.M. Gaffney for providing us the Gene Chips data of 41 primary HNSCC and 13 normal tissues, A. Imaoka for supporting microarray analysis, and Dr Kawai and Dr. Kitajima for helpful discussion.

References

1. Mao L, Hong WK, Papadimitrakopoulou VA. Focus on head and neck cancer. Cancer Cell 2004;5:311–6.
2. Fidler IJ. Critical factors in the biology of human cancer metastasis: twenty-eighth GHA Clowes Memorial Award Lecture. Cancer Res 1990;50:6130–8.
3. Kudo Y, Kitajima S, Sato S, Ogawa I, Miyauchi M, Takata T. Establishment of an oral squamous cell carcinoma cell line with high invasive and p27 degradation activity from lymph node metastasis. Oral Oncol 2003;39:515–20.
4. Kudo Y, Kitajima S, Ogawa I, et al. Invasion and metastasis of oral cancer cells require methylation of E-cadherin and/or degradation of membranous β-catenin. Clin Cancer Res 2004;10:5455–63.
5. Kudo Y, Ogawa I, Kitajima S, et al. Periostin promotes invasion and anchorage-independent growth in the metastatic process of head and neck cancer. Cancer Res 2006;66:6928–35.
6. Chen YX, Welte K, Gebhard DH, Evans RL. Induction of T cell aggregation by antibody to a 16kd human leukocyte surface antigen. J Immunol 1984;133:2496–501.
7. Takahashi S, Doss C, Levy S, Levy R. TAPA-1, the target of an antiproliferative antibody, is associated on the cell surface with the Leu-13 antigen. J Immunol 1990;145:2207–13.
8. Bradbury LE, Kansas GS, Levy S, Evans RL, Tedder TF. The CD19/CD21 signal transducing complex of human B lymphocytes includes the target of antiproliferative antibody-1 and Leu-13 molecules. J Immunol 1992;149:2841–50.
9. Matsumoto AK, Martin DR, Carter RH, Klickstein LB, Ahearn JM, Fearon DT. Functional dissection of the CD21/CD19/TAPA-1/Leu-13 complex of B lymphocytes. J Exp Med 1993;178:1407–17.
10. Deblandre GA, Marinx OP, Evans SS, et al. Expression cloning of an interferon-inducible 17-kDa membrane protein implicated in the control of cell growth. J Biol Chem 1995;270:23860–6.
11. Schor SL, Schor AM, Rushton G, Smith LJ. Adult, foetal and transformed fibroblasts display different migratory phenotypes on collagen gels: evidence for an isoformic transition during foetal development. Cell Sci 1985;73:221–34.
12. Kitajima S, Kudo Y, Ogawa I, et al. Role of Cks1 overexpression in oral squamous cell carcinomas: cooperation with Skp2 in promoting p27 degradation. Am J Pathol 2004;165:2147–55.
13. Kalebic T, Williams JE, Talmadge JE, et al. A novel method for selection of invasive tumor cells: derivation and characterization of highly metastatic K1735 melanoma cells based on *in vitro* and *in vivo* invasive capacity. Clin Exp Metastasis 1998;6:301–18.
14. Yuan B, Latek R, Hossbach M, Tuschl T, Lewitter F. siRNA Selection Server: an automated siRNA oligonucleotide prediction server. Nucleic Acids Res 2004;32:W130–4.
15. Guardavaccaro D, Kudo Y, Boulaire J, et al. Control of meiotic and mitotic progression by the F-box protein β-Trcp1 *in vivo*. Dev Cell 2003;4:799–812.
16. Elbashir SM, Harborth J, Lendeckel W, Yalcin A, Weber K, Tuschl T. Duplexes of 21-nucleotide RNAs mediate RNA interference in cultured mammalian cells. Nature 2001;411:494–8.
17. Ginos MA, Page GP, Michalowicz BS, et al. Identification of a gene expression signature associated with recurrent disease in squamous cell carcinoma of the head and neck. Cancer Res 2004;64:55–63.
18. Levy S, Todd SC, Maecker HT. CD81 (TAPA-1): a molecule involved in signal transduction and cell adhesion in the immune system. Annu Rev Immunol 1998;16:89–109.
19. Lickert H, Cox B, Wehrle C, Taketo MM, Kemler R, Rossant J. Dissecting Wnt/β-catenin signaling during gastrulation using RNA interference in mouse embryos. Development 2005;132:2599–609.
20. Andreu P, Colnot S, Godard C, et al. Identification of the IFITM family as a new molecular marker in human colorectal tumors. Cancer Res 2006;66:1949–55.
21. Behrens J, von Kriss JP, Kuhl M, et al. Functional interaction of beta-catenin with the transcription factor LEF-1. Nature 1996;382:638–42.
22. Bashir T, Pagano M. Aberrant ubiquitin-mediated proteolysis of cell cycle regulatory proteins and oncogenesis. Adv Cancer Res 2003;88:101–44
23. Holmes DI, Wahab NA, Mason RM. Cloning and characterization of ZNF236, a glucose-regulated Kruppel-like zinc-finger gene mapping to human chromosome 18q22–23. Genomics 1999;60:105–9.
24. Deryugina EI, Quigley JP. Matrix metalloproteinases and tumor metastasis. Cancer Metastasis Rev 2006;25:9–34.
25. Yang Y, Lee JH, Kim KY, et al. The interferon-inducible 9-27 gene modulates the susceptibility to natural killer cells and the invasiveness of gastric cancer cells. Cancer Lett 2005;221:191–200.
26. Owens DM, Watt FM. Influence of β1 integrins on epidermal squamous cell carcinoma formation in a transgenic mouse model: $\alpha3\beta1$, but not $\alpha2\beta1$, suppresses malignant conversion. Cancer Res 2001;61:5248–54.
27. Berditchevski F, Zutter MM, Hemler ME. Characterization of novel complexes on the cell surface between integrins and proteins with 4 transmembrane domains (TM4 proteins). Mol Biol Cell 1996;7:193–207.
28. Silvie O, Rubinstein E, Franetich JF, et al. Hepatocyte CD81 is required for Plasmodium falciparum and Plasmodium yoelii sporozoite infectivity. Nat Med 2003;9:93–6.